ISSN 1027-5495. Functional Materials, 27, No.4 (2020), p. 730-735.
doi:https://doi.org/10.15407/fm27.04.730

Electrochemical analysis of corrosion process of steel bar in fluid simulating porous concrete

F.Jiang, G.Jiang, W.Song, K.Zhu, N.He

College of information engineering, Dalian Ocean University,
116023 Dalian, China

Received September 3, 2020

Steel bar and concrete are the most commonly used materials in the construction industry, but the corrosion of steel bar has always been an unavoidable and urgent problem in the industry. The method of adding 0.12 mol chloride ion to a fluid simulating porous concrete with a pH value of 12.6 was used in the experiment. By analyzing the change of corrosion potential during steel bar erosion, the whole corrosion process was divided into four processes: passivation, depassivation, corrosion stabilization and corrosion deterioration; the potentiodynamic polarization curves, electrochemical impedance spectroscopy and their parameters were analyzed. According to the Nyquist impedance spectra of corrosion state and different equivalent circuits, the rules of passive film impedance, charge transfer resistance and double-layer capacitance on the surface of steel bar during the whole corrosion process were obtained.

Keywords: steel bar, porous concrete fluid, corrosion process, electrochemical impedance.

Електрохімічний аналіз процесу корозії сталевого стрижня у рідині, що моделює пористий бетон. *F.Jiang, G.Jiang, W.Song, K.Zhu, N.He*

Досліджується корозія сталевого стрижня у рідині, що моделює пористий бетон. В експерименті використано метод додавання 0,12 моль хлорид-іона до модельованої рідини пористого середовища бетону зі значенням pH=12,6. При аналізі зміни потенціалу корозії під час ерозії сталевого стрижня весь процес корозії розділено на чотири процеси: пасивація, депасивація, стабілізація корозії і корозійне руйнування, проаналізовано криві потенціодинамічної поляризації, спектроскопія електрохімічного імпедансу і їх параметри. За спектрами імпедансу Найквиста корозійного стану та різними схемами заміщення отримано правила імпедансу пасивної плівки, опору переносу заряду і ємності подвійного шару на поверхні сталевого стрижня протягом всього процесу корозії.

Исследуется коррозия стального стержня в жидкости, моделирующей пористый бетон. В эксперименте использовался метод добавления 0,12 моль хлорид-иона к жидкости, моделирующей среду пористого бетона со значением pH=12,6. При анализе изменения потенциала коррозии во время эрозии стального стержня весь процесс коррозии разделен на четыре процесса: пассивация, депассивация, стабилизация коррозии и коррозионное разрушение, проанализированы кривые потенциодинамической поляризации, спектроскопия электрохимического импеданса и их параметры. По спектрам импеданса Найквиста коррозионного состояния и различным схемам замещения получены правила импеданса пассивной пленки, сопротивления переносу заряда и емкости двойного слоя на поверхности стального стержня в течение всего процесса коррозии.

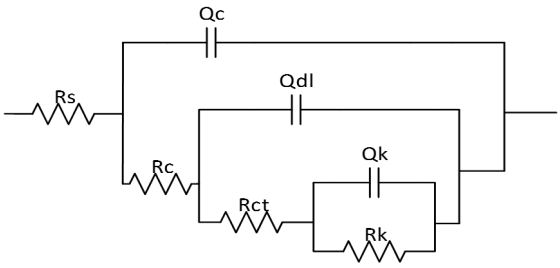

Fig. 1. Equivalent circuits of three time constants.

1. Introduction

As the most important architectural form in the world, reinforced concrete structures are widely used in every corner of people's life. At the same time, as plenty of basic materials for infrastructure, the durability of reinforced concrete is related to people's life safety and the life cycle cost of the building itself. A large number of researches have indicated that over time the passive film will be damaged due to low pH and free chloride ion penetration due to carbonization, leading to a loss of its protective effect on the steel bar and gradual corroding the surface. Therefore, it is of great significance to study the durability of the steel bar [1–5].

At present, the electrochemical impedance spectroscopy (EIS) is an important tool in the study of the structure and properties of materials. Generally, hardened cement paste in concrete can be regarded as an electrochemical system of a porous medium [6, 7]. Therefore, by measuring the electrochemical impedance spectra of concrete, the change in the microstructure of concrete can be effectively revealed. The equivalent circuit diagram intuitively expresses the process described above. Three common time constant equivalent circuits are shown in Fig. 1 [8–10].

In essence, the corrosion process of steel bars in concrete is an electrochemical reaction process. Concrete becomes an electrical conductor due to the movement of bound ions in one direction. In general, the corrosion of steel bars in concrete is due to natural electrochemical corrosion. A passive film for the steel bar can effectively protect it from corrosion, and the electromotive force here is different from that of the corroded steel bar. Therefore, the corrosion state can be estimated on the basis of the corrosion potential of the steel bar.

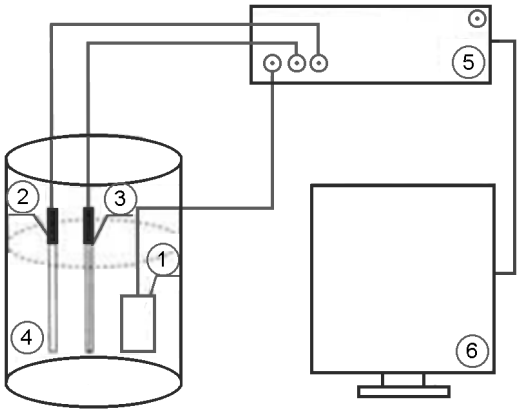

Fig. 2. Test scheme for the three electrode system.

2. Experimental

The working frequency of the electrochemical analyzer ranges from 10 mHz to 100 kHz, and the amplitude of the AC excitation signal is 10 mV. For the electrochemical test of carbon steel reinforcement and alloy steel reinforcement, the impedance spectrum was measured by a three-electrode system. As shown in Fig. 2, the 1 position is the test sample, and the steel bar blocks of carbon steel and stainless steel are measured in the experiment. The test sample 1 is connected with the working electric level of the electrochemical analyzer. The 2 position shows the auxiliary electrode and platinum electrode used. The 3 position is a saturated calomel electrode (SCE), and 4 is a reference electrode located as close as possible to the working electrode in the test. Then a computer 6 is connected with an electrochemical testing instrument 5 for data import and recording. The composition of the simulated porous fluid is shown in Table 1.

3. Results and analysis

3.1. Change of corrosion potential of steel bar with immersion time

The pH value in the simulated porous fluid was fixed at 12.6, and 0.12 mol/L sodium chloride was added. Fig. 3 shows the corrosion potential value of steel bar in the simulated porous fluid from day 1 to 81, and the corrosion potential and electrochemical impedance are measured each 2–3 days during this period. It is observed that the corrosion potential of the steel bar in the simu-

Table 1. Simulated porous fluid composition ($mol \cdot L^{-1}$)

pH	KOH	NaOH	$Ca(OH)_2$	$NaHCO_3$
12.6	0.06	0.02	0.0001	0.0242

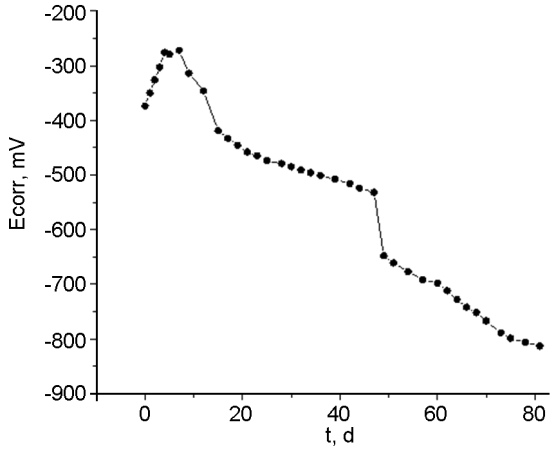

Fig. 3. Corrosion potential change with exposure time.

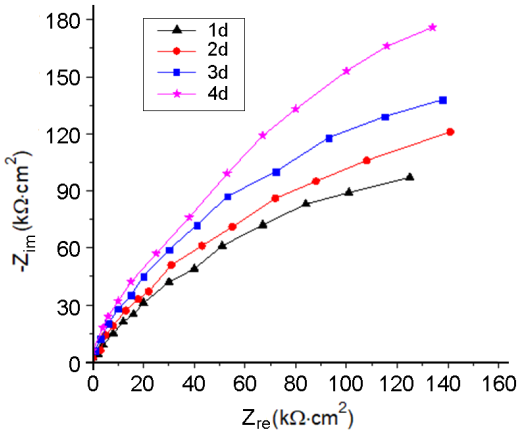

Fig. 4. Nyquist impedance spectrum of steel passivation process.

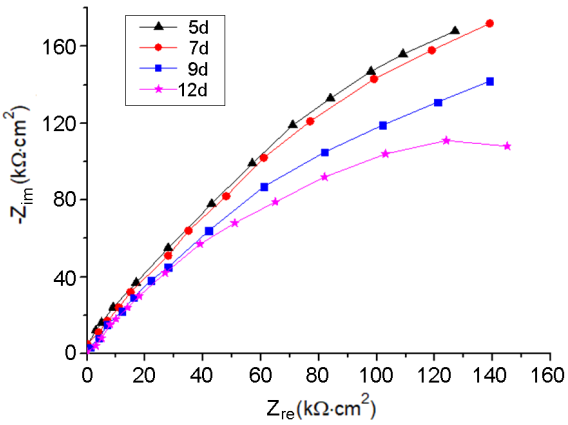

Fig. 5. Nyquist impedance spectrum of steel corrosion initiation process.

lated porous fluid increases in the initial stage, and then decreases to its lowest level at the 81st day. From the 1st to 4th day, the corrosion potential is in the positive shift stage, forming a stable passive film to protect the steel bar from chloride ion erosion. From the 4th to 7th day, the corrosion potential is stable at −270 mV. Although chloride ions have eroded the steel bar to some extent, the steel bar is still in the passivation stage and has a certain protective effect. From the 7th to 12th day, the corrosion potential continues to decrease and depassivation occurs. Over time, the chloride ion continuously corrodes the steel bar. When the passive film is damaged locally, pitting corrosion occurs. On the 15th and 49th days, the corrosion potential significantly decreases to −419 mV and −648 mV, respectively, and the corrosion is aggravated. Therefore, the corrosion process of the steel bar can be divided into four processes: passivation, corrosion initiation, corrosion stabilization and corrosion deterioration.

3.2. Electrochemical impedance spectroscopy characteristics of passivation process of steel bar

Fig. 4 shows the change of the Nyquist impedance spectrum of the steel bar passivation process in the simulated porous fluid. Over days, the radius of capacitive reactance arc increases, and a passive film gradually forms on the steel bar. The fitting parameters of the equivalent circuit are shown in Table 2. The resistance of the passive film R_c increases from 167 kΩ·cm^2 to 334 kΩ·cm^2.

3.3. Characteristic analysis of electrochemical impedance spectra during corrosion initiation of steel bars

Fig. 5 shows the Nyquist impedance curves on the 5th, 7th, 9th and 12th days in the soaking time range of 5–12 days. It can be seen that all curves of the impedance spectrum represent a capacitive reactance arc, and the capacitive reactance arc decreases with increasing soaking time of steel bars. The radius of the capacitive reactance arc on the 5th day is similar to that of the 7th day. It can be seen that in the range of 5–7 days, the passive film on the surface of steel bars remains intact and is in the passivation state, while in the period of 9–12 days, the radius of capacitive reactance arc decreases obviously, that is, the steel bars begin to degrade with chlorine ions and pitting occurs gradually. The passive film resistance R_c decreases from

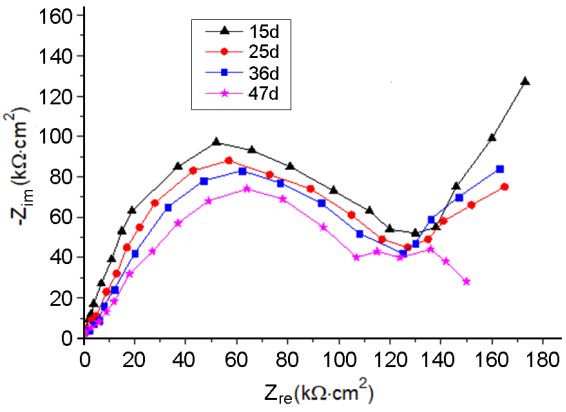

Fig. 6. Nyquist impedance spectrum of steel.

Table 2. Equivalent circuit parameters of electrochemical impedance in the passivation stage

Day	R_s, Ω·cm^2	Q_c, uF·cm^{-2}	n	R_c, kΩ·cm^2
1	22.2	1.82	0.97	167
2	36.5	2.24	0.96	203
3	24.3	1.75	0.96	242
4	12.9	1.47	0.94	334

320 kΩ·cm^2 to a minimum of 211 kΩ·cm^2. It can be concluded that the passive film is gradually destroyed, the resistance of the passive film decreases, the protective effect on the reinforcing matrix is weakened, and the pitting phenomenon gradually begins to occur.

3.4. Analysis of electrochemical characteristics of corrosion stabilization process of steel bar

Fig. 6 shows the Nyquist impedance diagram curves on 15th, 25th, 36th and 47th day. Over this time, the impedance spectrum changed from one capacitive reactance arc to two capacitive reactance arcs during the corrosion initiation process. That is, the impedance characteristics consist of two time constants, one in the high frequency region and the other in the low frequency region. The appearance of the second capacitive reactance arc in the low frequency region indicates that the sodium chloride in the solution gradually began to stimulate local corrosion. The process of charge transfer takes place on the surface of steel bars, and a double electric layer gradually forms on the surface of steel bars. The corrosion process of steel bars can be revealed by the resistance of the charge transfer process. The equivalent circuit is shown in Fig. 7,

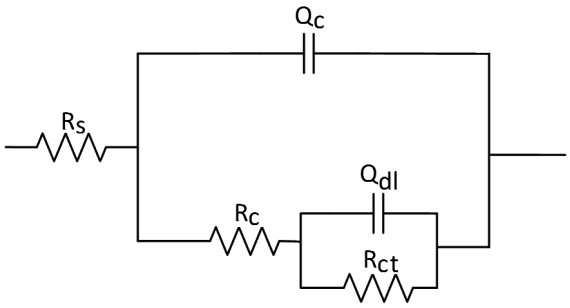

Fig. 7. Equivalent circuit of Nyquist impedance diagram for steel bar during corrosion.

Table 3. The equivalent circuit parameters of electrochemical impedance in the corrosion initiation process

Day	R_s, Ω·cm^2	Q_c, uF·cm^{-2}	n	R_c, kΩ·cm^2
5	124.2	2.22	0.95	327
7	152.9	4.13	0.96	314
9	98.6	6.54	0.95	244
12	113.3	5.47	0.93	211

where R_c is the passive film resistance, Q_c is the passive film capacitance, R_{ct} is the low-frequency half-circle charge transfer resistance, and Q_{dl} is the double-layer capacitance. The values of each parameter in the equivalent circuit are small as shown in Table 4.

From Table 4, it can be seen that the passive film resistance R_c gradually decreases from 192 kΩ·cm^2 on the 15th day to 166 kΩ·cm^2 on the 47th day. This is because during depassivation on the surface of steel bars, chloride ions combine with cations in the passive film to form soluble halides, which gradually destroy the steel bars. Compared with the previous corrosion initiation stage, the resistance of the passive film is lower, the pitting corrosion of steel bar develops into a state of localized corrosion, and the protective effect of the passive film on the steel bar becomes gradually weaker. The charge transfer resistance R_{ct} decreases from 69 kΩ·cm^2 on 15th day to 39 kΩ·cm^2 on 47th day. With the continuous corrosion of steel bars, corrosion gradually goes into a local range. As the corrosion continues, steel bars gradually loosen, the corrosion gradually accelerates, and the charge transfer resistance becomes less. From Fig. 6, it is obvious that the radius of the second low frequency circle decreases with an increase in the immersion time,

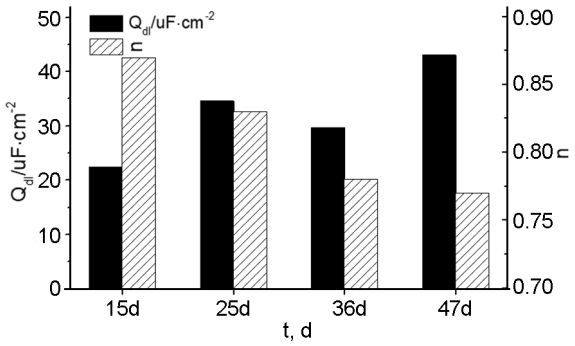

Fig. 8. Double-layer capacitance and index of steel surface.

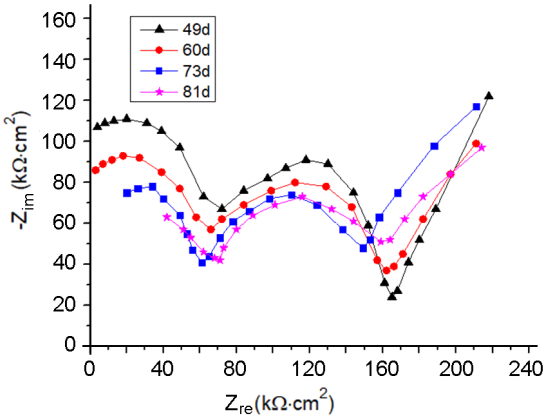

Fig. 9. Nyquist impedance spectrum of steel corrosion deterioration process.

that is, the charge transfer resistance of the equivalent circuit of steel bar in the simulated porous fluid decreases.

In Fig. 8, the change curves of double-layer capacitance Q_{dl} on the surface of steel bar and the dispersion index n are shown. They are also important parameters to characterize the corrosion of steel bar. The value of the double-layer capacitance Q_{dl} on the surface of steel bar gradually increases with corrosion from 22.5 uF on the 15th day to 43.1 uF. The n value decreases from 0.87 on the 15th day to 0.77. This is mainly due to the fact that the dispersion index n characterizes the smoothness of the surface of the entire system. As the degree of corrosion increases, the surface roughness of the steel bar increases and the value of n decreases, that is, the value of n will be further and further away from 1, so the dispersion effect becomes stronger.

3.5. Analysis of electrochemical characteristics of corrosion deterioration process of steel bars

Figure 9 shows the Nyquist impedance spectrum of a steel bar during corrosion deterioration in a porous simulation fluid when the holding time is 49–81 days. The Nyquist impedance spectrum shows two arcs and a straight line section with a larger arc that looks like an oblique line. The impedance spectrum shows a diffusion tail. At this time, the corrosion process gradually develops into a diffusion process. The equivalent circuit is shown in Fig. 10; R_k and Q_k are, respectively, the shunt resistance and capacitance introduced in the diffusion process at low frequency. The values of each parameter are shown in Table 5.

Table 5 shows that the passive film resistance R_c decreases from 103 kΩ·cm^2 on the 49th day to the minimum value of 33 kΩ·cm^2 on the 81st day. The resistance of the passive film can characterize the degree of corrosion due to the intensification of local corrosion of steel bar. The value of 33 kΩ·cm^2 of the passive film resistance on the 81st day indicates that the steel bar immersed in simulating porous fluid has reached the state of maximum deterioration. The charge transfer resistance R_{ct} decreases from 34 kΩ·cm^2 on the 49th day to the minimum value of 13 kΩ·cm^2 on the 81st day. Compared with the stable stage of corrosion, the degree of corrosion is further increased. As the degree of corrosion increases, the entire steel structure becomes looser, more chlorine ions are in contact with the steel bar, and the corrosion rate is higher than before, which reduces the charge transfer resistance.

Fig. 11 shows the curves of changing the double-layer capacitance Q_{dl} on the surface of steel bars and the dispersion index n, which are also important parameters to

Table 4. Electrochemical impedance equivalent circuit parameters in corrosion stabilization stage

Day	R_s, Ω·cm^2	Q_c, uF·cm^{-2}	n	R_c, kΩ·cm^2	Q_{dl}, uF·cm^{-2}	n	R_{ct}, kΩ·cm^2
15	56.2	5.9	0.72	192	22.5	0.87	69
25	74.5	8.3	0.78	179	34.6	0.83	57
36	82.9	7.4	0.86	133	29.7	0.78	44
47	44.6	11.8	0.73	121	43.1	0.77	39

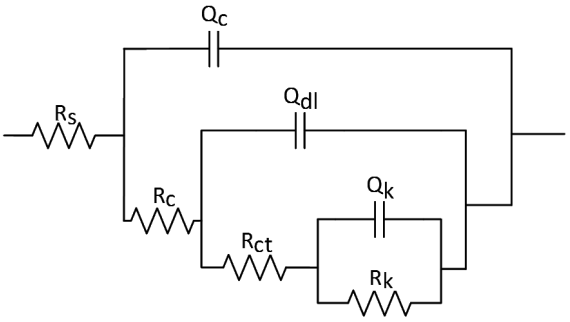

Fig. 10. Equivalent circuit of Nyquist impedance diagram for steel bar during corrosion deterioration process.

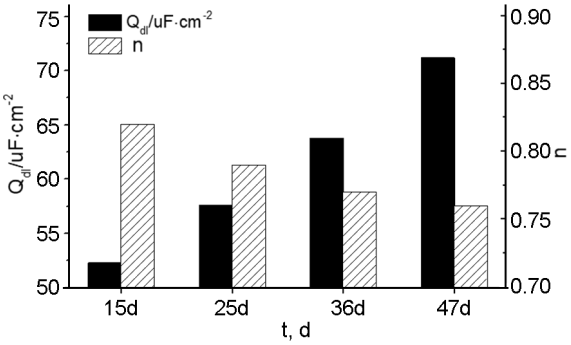

Fig. 11. Values Q_{dl} and n on the steel bar surface.

Table 5. Electrochemical impedance equivalent circuit parameters in corrosion deterioration stage

Day	R_s, $\Omega \cdot cm^2$	Q_c, $uF \cdot cm^{-2}$	n	R_c, $\Omega \cdot cm^2$	Q_{dl}, $uF \cdot cm^{-2}$	n	R_c, $\Omega \cdot cm^2$	Q_k, $uF \cdot cm^{-2}$	n	R_k, $k\Omega \cdot cm^2$
49	47.3	4.4	0.83	103	52.3	0.82	34	5	0.89	12
60	54.6	7.8	0.79	92	57.6	0.79	25	8	0.77	15
73	38.9	14.5	0.62	48	63.8	0.77	18	7	0.82	14
81	43.1	12.9	0.73	33	71.2	0.76	13	4	0.85	17

characterize the corrosion of steel bars. As can be seen from Fig. 11, compared with the previous stable stage of corrosion of the steel bar, the double-layer capacitance Q_{dl} on the surface of the steel bar continues to increase from 52.3 uF on the 49th day to 71.2 uF, indicating that corrosion is worsening. The index n decreases gradually from 0.82 on the 49th day to 0.76. It can be seen that the dispersion index n of the double-layer capacitance Q_{dl} on the surface of steel bar is farther from 1, the corrosion deepens further and the surface of steel bars becomes rougher.

4. Conclusions

The passive film resistance R_c decreases gradually with an increase in the steel corrosion degree. The surface corrosion of steel bars undergoes four stages: from local pitting to pitting, then to local corrosion, and finally to deterioration of steel bars as a whole. The radius of the capacitive reactance arc in the Nyquist impedance spectrum increases continuously. With an increase in the corrosion time to 47 days, two capacitive reactance arcs appear. At the stage of aggravating corrosion of a steel bar, a diffusion tail of a straight section appears in the impedance spectrum as an oblique line.

Acknowledgements. Natural Science Foundation of Liaoning Province (No.2019-ZD-0731), Financial supports from Liaoning Provincial Department of Education Project (No.QL201717, No.QL201913) are gratefully acknowledged.

References

1. Shi Meilun, Concrete Impedance Spectrum, China Railway Publishing House, Beijing (2003).
2. Zhou Qun, Shui Zhong He, XiaoYi De et al., *Adv. Mater. Res.*, **446–449**, 3176 (2012).
3. Ming Liu, Xuequn Cheng, *J. Electroanal. Chem.*, **7**, 803 (2017).
4. Gjorv, E.Odd, Durability Design of Concrete Structures in Severe Environments, Sec. Ed., Deterioration, 629 (2014).
5. Lai Jianzhong, Yang Chunmei, Cui Chong, Zhu Yaoyong, *Silicate J.*, **11**, 1592 (2012).
6. Jiang Fengjiao, Gong Jinxin, Zhu Jichao et al., *Intern. J. Pattern Recogn. Artificial Intelligence*, 6 (2020).
7. J.Tritthart, K.Pettersson, *Cement & Concrete Res.*, **23**, 10954 (1993).
8. Chen Y, Xia C, Shepard Z, et al., *ACS Sustainable Chem. Engin.*, **5(5)**, 3955 (2017).
9. Wang Wei, Qian Liang, Zhang Yu et al., in: Proc. of IOP Conference Series: Earth and Environmentalence, v.267 (2019).
10. Jiang Fengjiao, Gong Jinxin, Zhang Wen, *J. Xi'an Univ. Architect. Techn.*, **4**, 493 (2016).